FOCUSED ISSUE FEATURE

NVNA Techniques for Pulsed RF Measurements

Patrick Roblin, Young Seo Ko, Chieh Kai Yang, Inwon Suh, and Seok Joo Doo

With the advent of nonlinear vector network analyzers (NVNA), new measurement techniques have become available for characterizing nonlinear radio-frequency (RF) devices and circuits. In particular, the accurate measurement of the response of nonlinear circuits to periodic modulated and pulsed nonlinear RF excitation is now possible. Furthermore, using advanced triggering and multiple recording techniques, 1) the implementation of a real-time (ultra fast) active load-pull, 2) the measurement of pulsed-RF, pulsed-bias signals with reduced desensitization, and 3) the measurement of phase-stable RF signals with very wide (gigahertz) modulation bandwidths have been demonstrated. These advanced measurement techniques are the subject of this article.

Three major types of NVNAs have been developed: sampler-based NVNAs, scope-based NVNAs and mixer-based NVNAs. Here, we focus on the sampler-based NVNAs, which include the original microwave transition analyzer (MTA) from Agilent, the large-signal network analyzer (LSNA) [1] from Maury Microwaves, and the recently commercialized Superfast WAve Processor (SWAP) from Verspecht-Teyssler-DeGroote (VTD), all shown in Figure 1. See [2] for a brief history of the development of sampler-based NVNA technology. The sampler-based NVNAs typically have a smaller dynamic range (on the order of 70 dB) but have the

Patrick Roblin (roblin@ece.osu.edu), Young Seo Ko, Chieh Kai Yang, Inwon Suh, and Seok Joo Doo are with the Nonlinear RF Group, ECE Department, Ohio State University.

Digital Object Identifier 10.1109/MMM.2010.940103
Date of publication: 9 March 2011

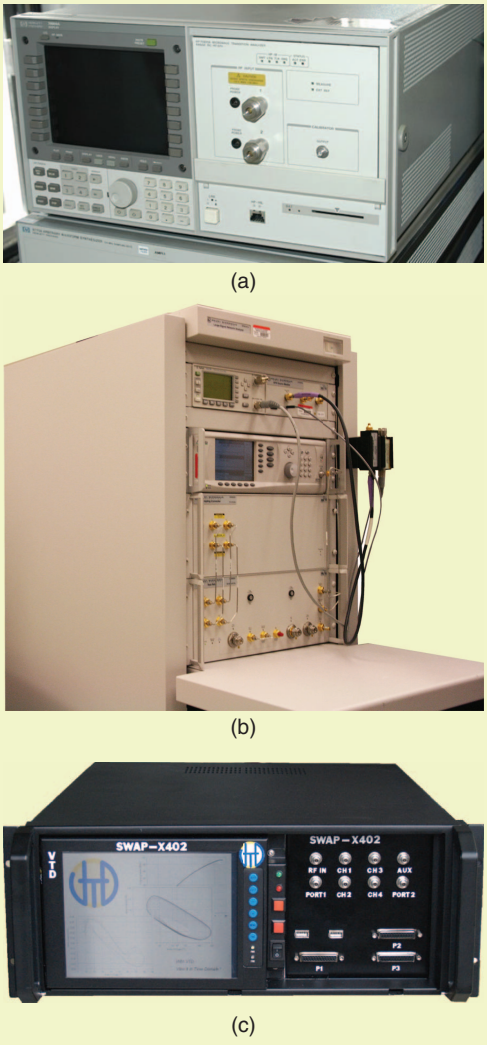

Figure 1. *Three generations of sampler-based nonlinear vector network analyzers (NVNAs): (a) the microwave transition analyzer (MTA) for measurement with sampling down conversion (1991, photo courtesy of Ke Wu, used with permission), (b) the large signal network analyzer (LSNA), which integrates two MTAs and harmonic phase reference calibration (1995, photo copyright Cambridge University Publishing, used with permission), and (c) the SWAP, a new sampler-based NVNA, which offers a low-cost instrument for dedicated large-signal measurements (2009, photo courtesy of Jean-Pierre Teyssier, used with permission).*

advantage of acquiring periodic continuous-wave (CW) and modulated RF signals in a single-measurement record (for example 10 ms for a 100 Hz resolution bandwidth). The phase accuracy is typically a fraction of a degree for a multisine with 64 tones of equal power [3]. Note that multisine excitations are often used for characterizing devices [4] because their periodic nature aligns to the frequency grid of sampler-based systems.

The sampler-based NVNA relies on sampling down-conversion to acquire, in a single measurement, the amplitude and phase of the fundamental and harmonics of the incident and reflected waves for periodic RF excitations. The RF signals can also be periodically modulated or pulsed. The principle of operation of subsampling is that of a stroboscope [1]. Subsampling essentially down-converts all the RF tones in the measurement bandwidth of the intermediate frequency (IF) receiver.

Sampling and Broadband Measurements

The sampler-based NVNA can acquire multitone periodic signals with wide RF bandwidth (up to 50 GHz in the LSNA) and effectively remap them under appropriate conditions within the bandwidth of its IF receiver (10 MHz in Maury's LSNA and 50 MHz in VTD's SWAP). Once down-converted to IF, the RF tones are filtered with a low-pass IF filter and then sampled and digitized using analog-to-digital converters (ADCs). See "Sampling Down-Conversion in a Sampler-Based NVNA" for a more detailed discussion.

In the first commercialized sampler-based NVNA, the modulation bandwidth for the RF signals acquired was initially limited to twice the IF receiver bandwidth, e.g., 20 MHz in the LSNA and 100 MHz in the SWAP. It is, however, possible under appropriate conditions to further increase the modulation bandwidth by a proper selection of the measurement parameters of the NVNA, such as the local oscillator (LO) sampling frequency and the ADC frequency, in such a way that none of the fundamental and harmonic tones fold down to the same IF-band frequency during down-conversion. Uncalibrated measurements of RF signals, with gigahertz bandwidth were first reported in [5]. Calibrated broadband measurements were next achieved by stitching several narrower band measurements [6]. Advanced ADC triggering techniques which enable one to acquire, in a single measurement, phase-stable broadband RF signals were then demonstrated for four tones by [7] and for 64 tones by [3] (see Figure 2) both at eight times the IF bandwidth of the LSNA receiver. To stabilize the phase, the ADC trigger frequency used for starting the measurements needs to be a subharmonic of the greatest common divider frequency for all the down-converted IF tones of interest [3]. The modified architecture required for this measurement is shown in Figure S1. The ADC trigger is generated from the ADC fractional-N (fracN) synthesizer (a highly precise and stable single-tone source with programmable frequency in the IF band) using a counter.

Pulsed-RF Measurements Using Broadband Acquisition

Pulsed-bias, pulsed-RF measurements are becoming common practice for the nonlinear characterization of microwave transistors that are affected by self-heating and trapping. Using a pulsed-bias and pulsed-RF

Sampling Down-Conversion in a Sampler-Based NVNA

A simplified architecture for the sampler-based NVNA is showed in Figure S1. As in a normal network analyzer, two couplers are used to separate the incident and reflected waves at ports 1 and 2. The sampler-based NVNA then relies on sampling-down conversion for measuring the amplitude and phase of these multiharmonic RF signals. Sampling-down conversion is illustrated in Figure S2. In the example, a sampling signal with a 9-MHz repetition (LO) frequency is used to sample a 1 GHz input RF signal with two harmonics. In the frequency domain, this sampling signal corresponds to a frequency comb with a 9 MHz tone spacing, which extends, typically, up to 50 GHz due to the very short pulse duration. In this example the 111th, 222nd, and 333rd harmonics of the LO frequency are used to down-convert the input RF signal to IF signals at 1, 2, and 3 MHz, respectively:

1 GHz tone: 1000 MHz − 111 × 9 MHz = 1 MHz
3 GHz tone: 2000 MHz − 222 × 9 MHz = 2 MHz
3 GHz tone: 3000 MHz − 333 × 9 MHz = 3 MHz.

The RF signals can be pulsed or periodically modulated. The LO frequency is then carefully selected so that none of the harmonics and sideband frequencies overlap, once down-converted to the IF bandwidth of the receiver. A one-to-one mapping of the RF tones in the IF band is then established, which essentially preserves the relative linear phase relation between the measured tones independent of the power level, as long as any distortion is avoided in the LSNA itself.

As in a normal network analyzer, a relative phase calibration is used to account for the phase shifts, losses and leakage exhibited by the couplers of the test set. This relative calibration determines the error correction matrix up to an arbitrary complex constant K_n for each harmonic $n\omega$. A power calibration with a power meter at each harmonic tone of interest is used next to determine the amplitude $|K_n|$, so that the absolute power level is measured for each harmonic. Finally, a harmonic phase reference (HPR) is used to measure the relative phase between the harmonics and the fundamental in order to establish the phase of the correction constant K_n for the harmonics ($n > 1$). See [2] for a more detailed discussion of the calibration of the sampler-based NVNA.

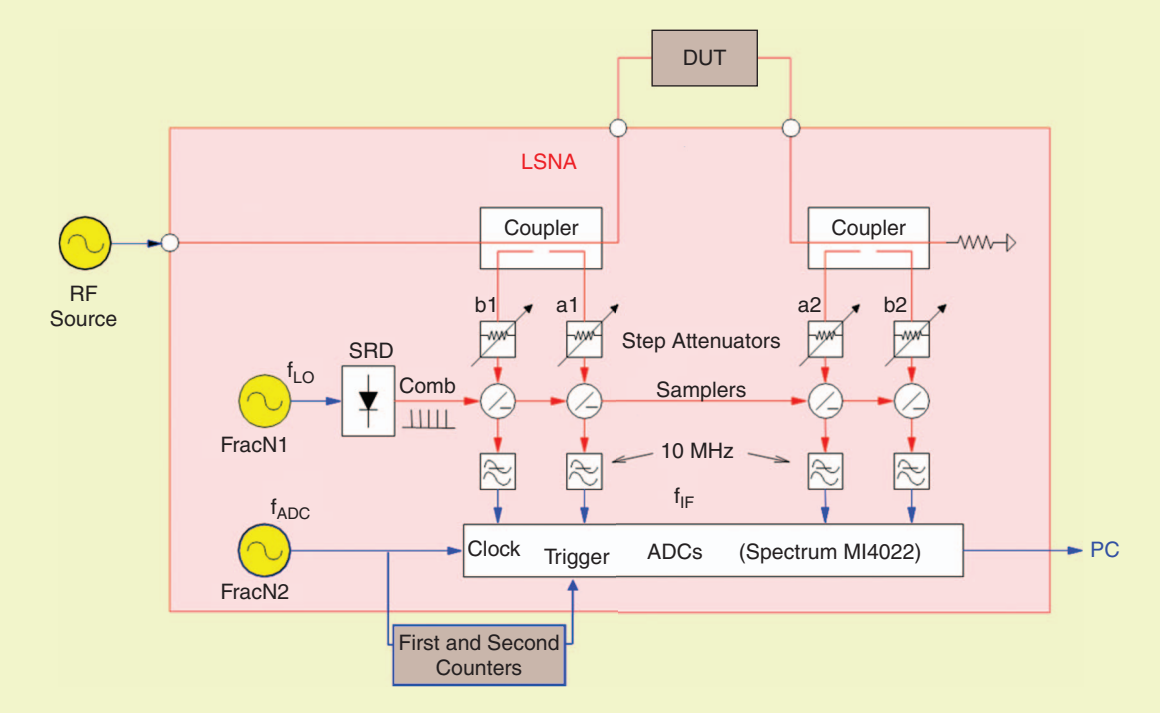

Figure S1. *Architecture for a sampler-based nonlinear vector network analyzer. A second fractional-N synthesizer (FracN2) is used in the system shown to control the analog-to-digital converter frequency as needed for broadband and multiple-recording measurements.*

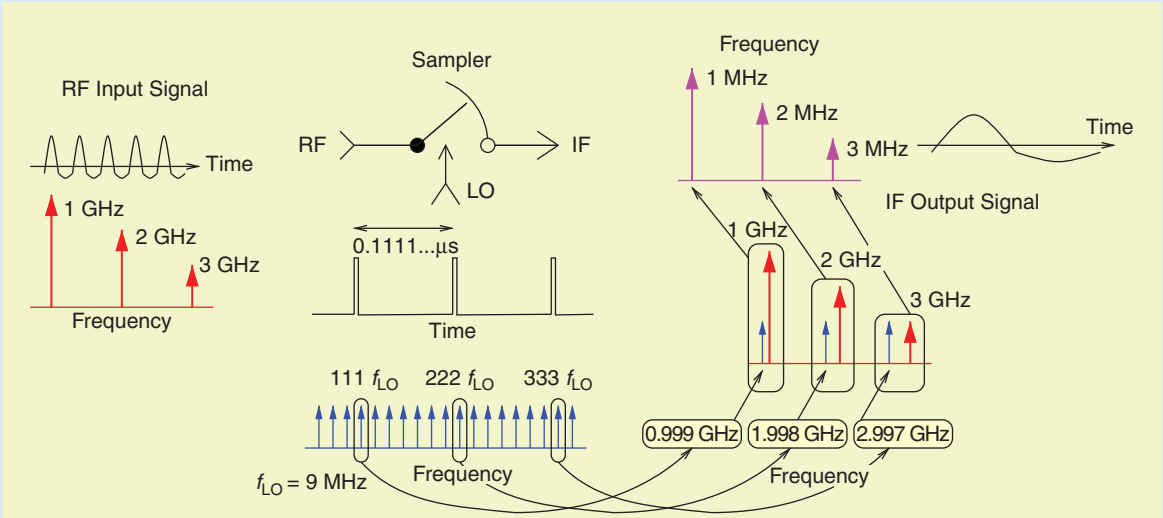

Figure S2. *Sampling with a sampler-based nonlinear vector network analyzer. A 1 GHz signal with two harmonics (2 and 3 GHz) is down converted by sampling with a 9-MHz sampling pulse to an intermediate frequency signal at 1 MHz with two harmonics (at 2 and 3 MHz).*

measurement, the isothermal RF response of a transistor can be obtained and the effect of traps mitigated. See [8] for a discussion of the measurement of pulsed-RF (small-signal) S-parameters with a vector network analyzer (VNA). Large-signal pulsed-RF measurements can also be pursued with NVNAs. Note that even though traps will not normally respond instantaneously to an RF signal, the average trap occupation will still depend on the dynamic load-line trajectory for large-signal excitations [9] due to cyclostationary effects. As was demonstrated in [10], the trap occupation is dependent on the time average (over an RF cycle) of the bias-dependent emission and capture rates along the periodic load-line trajectory.

An example of a pulsed-bias, pulsed-RF test bed is shown in Figure 3. Using an NVNA, a large fraction of

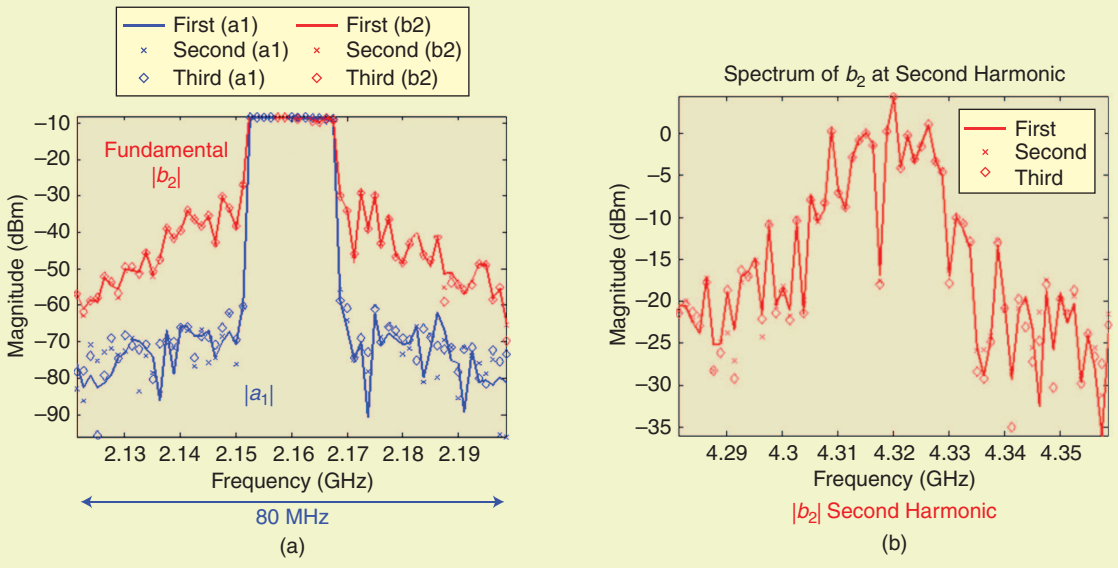

Figure 2. *Three successive single-record large-signal network analyzer measurements at eight times the intermediate frequency bandwidth of an 80-W average power AlGaN/GaN high electron mobility transistor (HEMT) Doherty power amplifier: (a) fundamental frequency and (b) second harmonic for a 13-tone multisine excitation. The output signal was normalized for comparison with the input signal.*

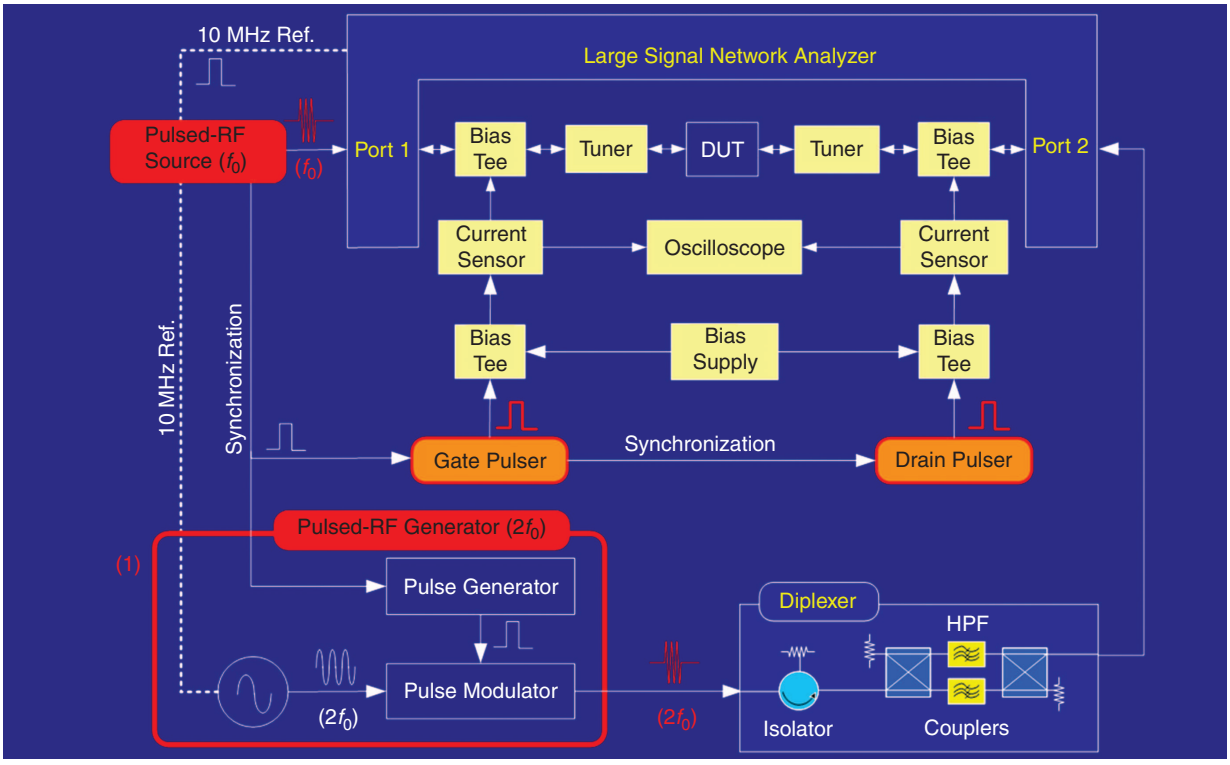

Figure 3. *Active load-pull test bed used for pulsed-RF, pulsed-bias measurements [12].*

the RF spectrum of the pulsed-RF signal can be acquired. The amplitude and phase acquired around the fundamental frequency for such a measurement are shown in Figure 4 [11]. The amplitudes take the shape of a sinc function. One can verify that 90.3% of the RF power is included in the center lobe of the sinc spectrum.

A key issue when measuring pulsed-RF signals is the desensitization of the test equipment. The desensitization can be defined as the ratio of the peak power of the pulsed-RF signal to the power of the signal actually measured by the test equipment:

$$\text{Desensitization(dB)} = 10\log\frac{\text{Peak Power}}{\text{Average Measured Power}}.$$

The desensitization is a measure of the effective reduction of the dynamic range of the test equipment. The attenuation level in the test equipment should be set such that the peak power of the measured signal does not exceed the damage level of the test equipment front end. Under pulsed operation, the dynamic range is therefore reduced by the desensitization:

$$\text{Pulse Dynamic Range (dB)} = \textit{CW}\ \text{Dynamic Range(dB)} - \text{Desensitization(dB)}.$$

Note that maintaining a high dynamic range is critical for detection of weak components (intermodulation products, spectral regrowth) of the signal and reduction of noise corruption.

Relative to the peak power, the average power for a pulsed signal is intrinsically reduced by a desensitization factor of $-10\log[\text{Duty Cycle}]$. When measuring only the main lobe (90.3% of the average power) with the NVNA, the desensitization is then

$$\text{Desensitization(dB)} = -10\log[\text{Duty Cycle}] - [0.903].$$

For a pulse duty cycle of 0.3%, this corresponds to a desensitization of 25.44 dB. If only the center tone is acquired with a conventional network analyzer, the desensitization is instead:

$$\begin{aligned}\text{Desensitization(dB)} &= 10\log\frac{\text{Peak Power}}{\text{Center Tone Power}}\\ &= -10\log[\text{Duty Cycle}^2]\\ &= -20\log[\text{Duty Cycle}].\end{aligned}$$

This corresponds to a desensitization of 50 dB for a duty cycle of 0.3%. It is greatly advantageous to acquire and use all the tones in the center lobe to avoid degrading the dynamic range of the sampler-based NVNA.

With this direct NVNA measurement technique, we can use all of the modulated RF tones (amplitudes and phases) acquired for the fundamental frequency band and harmonics to calculate the

It is possible, under appropriate conditions, to further increase the modulation bandwidth by a proper selection of the measurement parameters of the NVNA.

time-response of the device at the center of the RF pulses. As an example of the application of pulsed-RF pulsed-bias measurements, let us consider the acquisition of the dynamic RF load-lines of a GaN high electron mobility transistor (HEMT) with strong memory effects.

First, let us reproduce the CW experiment conducted by [14]. A GaN transistor suffering from strong knee walk-out (increasing knee voltage with increasing dc drain bias) is measured using pulsed-IV measurements. The pulsed-IV characteristics for the same pulsed gate voltage ($v_{GS} = 0$ V) are plotted in Figure 5 for different dc bias points (triangles with $V_{GS} = -2.5$ V and V_{DS} varying from 5, 7.5, and 12.5 V). The RF dynamic load-lines measured by an LSNA at 2 GHz for the same bias points are also shown. As the bias drain voltage V_{DS} increases, the RF drain current swing is seen to reduce and only reach the maximum current predicted by the pulsed IV characteristics with the same dc biasing point. Note that the RF gate voltage swing is from −5 V to 0 V in all these experiments.

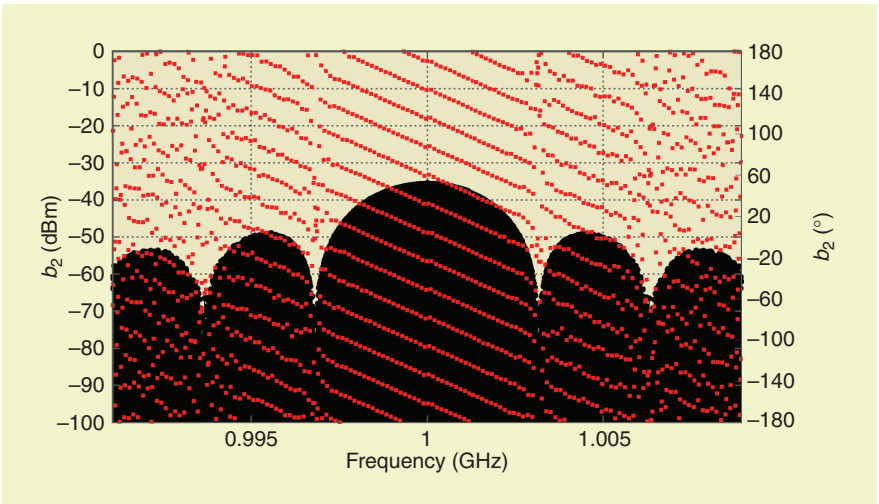

Figure 4. *Measured sinc spectrum associated with pulsed-RF signals measured at the fundamental frequency: (a) black stems are for the amplitudes and red squares for the phases. 90% of the RF power is located in the center lobe (From [13] with permission, ©2011 Cambridge University Press).*

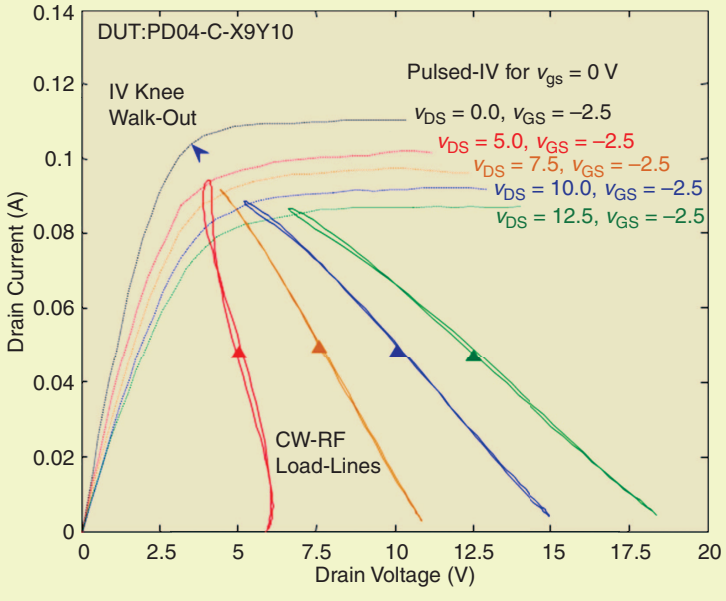

Figure 5. *CW RF load-lines for a GaN HEMT exhibiting knee walk-out compared to pulsed-IV characteristics from various dc bias points (measurements similar to [14]). 1% duty rate with 1 μs pulse duration is used for the pulsed-IV.*

Let us inspect now the response of the device under pulsed-bias, pulsed-RF excitation. The device is resting at $V_{GS} = 0$ and $V_{DS} = 0$ and is briefly pulsed to the various bias points (blue triangles on Figure 6). A 1% duty rate with 1 μs pulse duration is used for the bias voltage. An RF excitation with 0.3% duty rate and 0.3 μs pulse duration is then applied at the transistor input such that the gate voltage swing is again from −5 V to 0 V. The resulting RF dynamic load-lines [15] obtained from pulsed-bias/RF measurements are compared with those of the CW-RF case in Figure 6. In contrast to the CW-RF load-lines featuring a reduced current swing, the pulsed-bias, pulsed-RF dynamic load-lines exhibit a much larger current swing. Using the current swing as a metric, the IV knee walk-out is actually effectively suppressed. In this GaN HEMT on a sapphire substrate, the knee walk-out actually originates from self-heating. This can be verified since the undesirable IV knee walk-out, which is effectively suppressed in the pulsed-bias, pulsed-RF measurements,

is reintroduced if the substrate temperature is set to the surface temperature of the device in CW operation [15].

Pulsed-RF Measurements Using Multiple Recording Techniques

In the broadband measurement method discussed in the previous section, all of the tones within the main lobe of the signal (90% of the power) were acquired, enabling one to partially compensate for the loss of dynamic range by decreasing the desensitization by approximately half (in decibels). However, this method is still limited in practice to duty cycles equal or above 0.3%. As the number of tones increases for decreasing duty cycles, the peak RF power is spread among more tones, owing to the lower repetition frequency, and so the power level of the individual tones will eventually fall below the minimum detectable power level of the sampler-based NVNA, assuming the peak RF power is kept the same.

Recently, an alternative time-domain technique developed at XLIM [16]–[18] was reported for the sampler-based NVNA that allows for very low duty-cycles without any reduction in the dynamic range. This time-domain technique relies on the multiple recording capability of modern ADCs to control the acquisition of the sample data. A dedicated pulse control board was developed at XLIM to control the ADC acquisition such that the sampled, down-converted RF data from the sampler-based NVNA are only acquired at times where the RF pulse is applied. The principle of operation is illustrated in Figure 7. In this example, an RF signal with three harmonics is down-converted by subsampling to the IF signal represented by the red dots. Multiple recording is used to acquire this IF signal in four different records. In this example, the records are separated by one IF period. In practice, a large number of IF periods can be used without any spectral leakage to achieve very small duty-cycles, e.g., 0.01%. Also, to sample a narrow region of the RF/IV pulse, a small number of samples (one or two) is typically used.

Since the average power of the signal acquired is now the peak power of the pulsed signal, this modified LSNA data acquisition does not, theoretically, exhibit any degradation in dynamic range for decreasing pulse duty cycles.

With the advent of NVNAs, new measurement techniques have become available for characterizing nonlinear RF devices and circuits.

$$\text{Desensitization(dB)} = 10 \log \frac{\text{Peak Power}}{\text{Average Measured Power}} = 0 \text{ dB}.$$

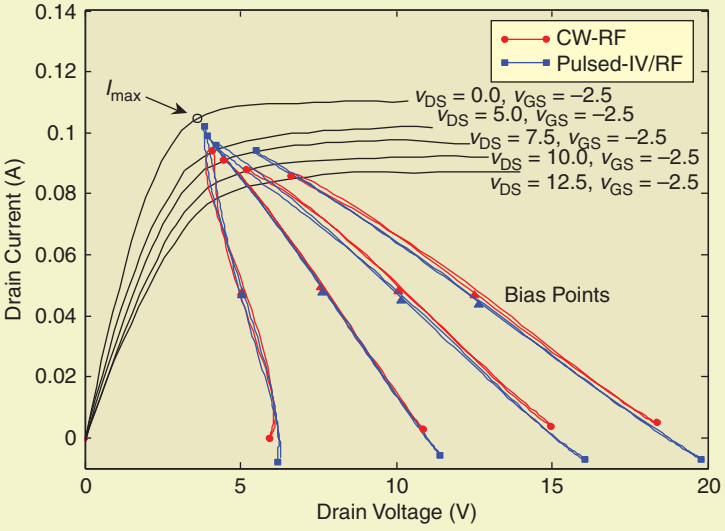

Figure 6. *Suppression of IV knee walk-out (blue lines) achieved by pulsing both the dc bias and the RF signal. Full current and voltage swings are recovered under pulsing, compared to the CW load-lines (red lines) [15].*

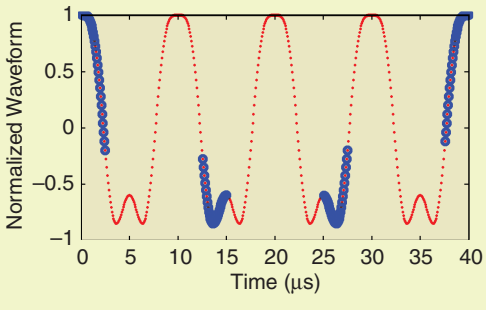

Figure 7. *Multiple recordings of a RF signal with three harmonics in four records with one IF period skipped. The blue circles represent the multiple recording samples and the red dots represent the IF signal being acquired. Smaller duty cycles can be obtained by skipping multiple IF periods. In pulsed-bias, pulsed-RF measurements, the input RF signal and dc bias are only applied during the recording period (blue circles) (from [13] with permission, ©2011 Cambridge University Press).*

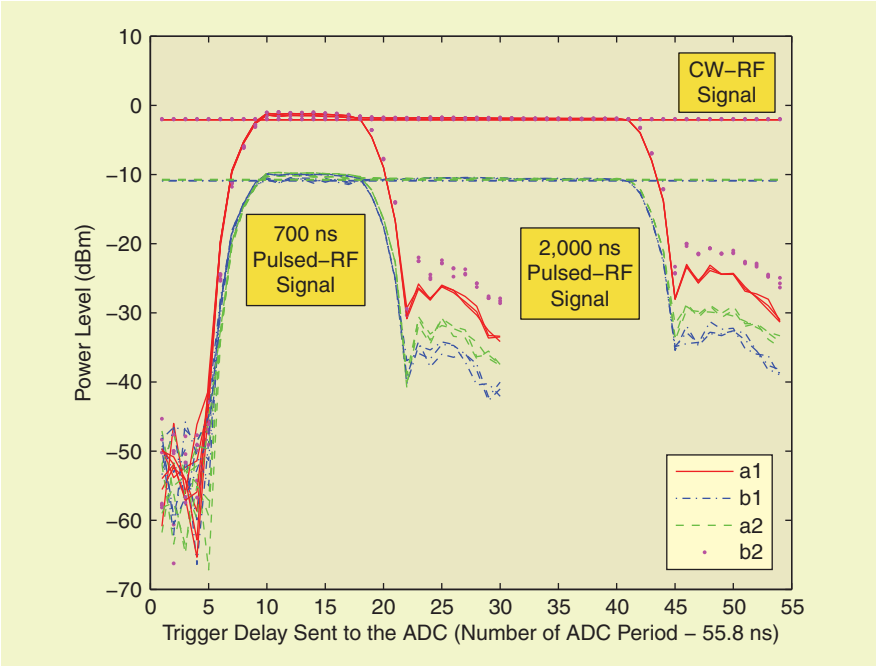

Figure 8. *Suppression of desensitization using multiple recordings [16], [17]. The pulsed-RF signals measured with different delays exhibit the same power levels (−2 dBm for a_1 and b_2 and −11 dBm for b_1 and a_2) as the CW signal (horizontal lines), independent of the duty cycle [19].*

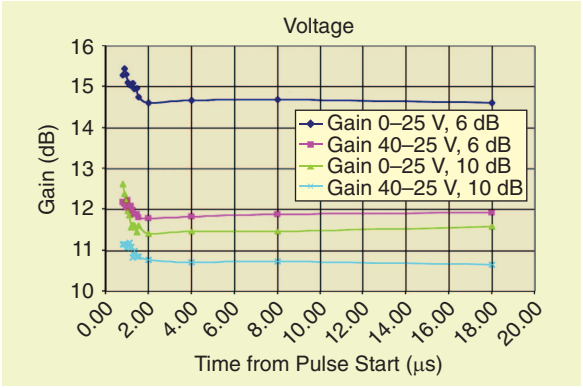

Figure 9. *Time-resolved power-gain for a GaN HEMT power amplifier excited by a pulsed-RF signal at 2 GHz while the drain voltage is pulsed to 25 V. The initial dc bias is either 0 or 40 V. The transistor is operated in the strongly nonlinear regime with a high gain compression of either 6 or 10 dB. The measurements are performed using multiple recordings with a large-signal network analyzer [18], (used with permission from the European Microwave Association).*

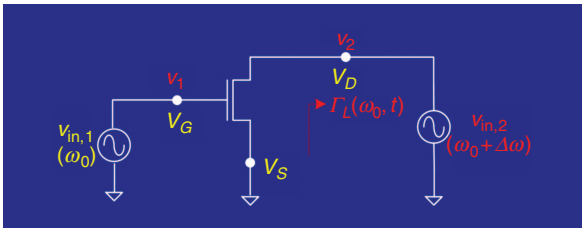

Figure 10. *Conceptual schematic for real-time active load-pull.*

This is demonstrated in Figure 8, where CW and pulsed-RF waves measured are compared. The resulting 0 dB desensitization is, however, achieved at the price of a longer measurement time and requires additional triggering hardware for the synchronization of the ADC data acquisition (Figure S1). Also, a relatively large latency 500 ns is observed in the LSNA IF filter/amplifier which currently prevents the measurement of RF pulses below 700 ns. New sampler-based NVNAs will remove this limitation. For example, in the SWAP, the latency is reduced to 50 ns.

Large-signal measurements can be conducted with the multiple recording scheme with increased time resolution (LSNA 40 ns, SWAP: 10 ns). For example, as is shown Figure 9, the time variation of the power gain of a GaN HEMT power amplifier (PA) has been measured using an LSNA shortly after an RF pulse at 2 GHz is applied to reveal the memory effects of the PA [18]. In this experiment, the drain voltage was pulsed to 25 V and a high input power level was used to drive the transistor into its nonlinear regime. The gain decrease was found to depend upon the level of the gain compression (6 and 10 dB) and the initial dc bias condition (0 or 40 V).

In addition, pulsed-RF small-signal measurements can be conducted using multiple recordings. The method was recently used with the cold-field effect transistor (FET) technique to extract the device parasitics as a function of dc biasing conditions in a transistor exhibiting memory effects [19].

Real-Time Active-Load-Pull with the Sampler-Based NVNA

Passive load-pull and active load-pull measurements are traditionally used by microwave engineers to design power amplifiers. See [8] for an excellent discussion on this topic and related power transistor characterization. Recently, a real-time active-load-pull technique using the NVNA has been introduced [20] which has the potential for drastically reducing the PA design cycle. Figure 10 shows a conceptual implementation for the first harmonic. An RF signal with an offset frequency $\Delta f = \Delta\omega/(2\pi)$ from the frequency ω_0 of the input RF signal is injected at the output.

The resulting load reflection coefficient $\Gamma_L(\omega_0, t)$ becomes effectively modulated in time and can be evaluated from the modulated incident $A_2(\omega_0, t)$ and reflected $B_2(\omega_0, t)$ waves measured at port 2:

$$\Gamma_L(\omega_0, t) \equiv \frac{A_2(\omega_0, t)}{B_2(\omega_0, t)} = \sum_{m=-M}^{M} a_2(\omega_0 + m\Delta\omega)e^{jm\Delta\omega t} \Big/ \sum_{m=-M}^{M} b_2(\omega_0 + m\Delta\omega)e^{jm\Delta\omega t},$$

where $a_2(\omega_0 + m\Delta\omega)$ and $b_2(\omega_0 + m\Delta\omega)$ are, respectively, the incident and reflected waves at the sideband tones $\omega_0 + m\Delta\omega$ around the fundamental frequency ω_0. The resulting loci of the modulated reflection coefficients are shown on Figure 11 for a 65 nm metal-oxide semiconductor FET (MOSFET) for several real-time active-load-pull measurements with different output power levels. Real-time active load-pull permits one to rapidly map the Smith Chart in a few 10 ms measurements.

The resulting constant output power contours for this 65 nm MOSFET are shown in Figure 12 for the fundamental frequency. One of the potential drawbacks of real-time active load-pull is that the impedance sweeping may trigger memory effects (trapping and self-heating) in the transistors. The memory effects can be detected by performing measurements with different modulation frequencies. The accuracy of the real-time active load-pull measurements can also be verified by using a conventional active load-pull around the optimum point predicted by the real-time active load-pull. Alternately, we shall see in the following that real-time active load-pull can be combined with pulsed-RF measurements to reduce, if not eliminate, memory effects.

Multiharmonic Real-Time Active Load-Pull

The real-time active-load-pull technique which was first demonstrated for the fundamental frequency can also be extended to higher-harmonic load-pull measurements for the interactive design of high-efficiency, class F (see [21]) power amplifiers [22], [23]. A test-bed implementation for the fundamental and the second and third harmonics is shown in Figure 13. An example of second-harmonic real-time active load-pull results is shown in Figure 14 for the optimization of the output power of a negative resistance oscillator [24].

Device Modeling Using Real-Time Active-Load-Pull

Returning to the 65 nm complimentary MOSFET (CMOSFET), it is interesting to note that within a single LSNA measurement of 10 ms (100 Hz resolution frequency), the dynamic load-line experienced

A dedicated pulse control board was developed at XLIM to control the ADC acquisition such that the sampled, down-converted RF data from the sampler-based NVNA are only acquired at times where the RF pulse is applied.

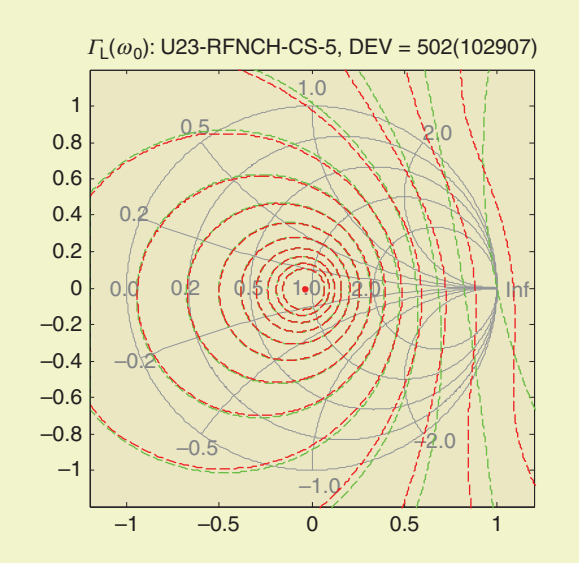

Figure 11. *Reflection coefficient loci from a real-time active-load-pull measurement for different output power levels. The green and red lines are the loci obtained when the higher intermodulation products of the dominant tones at f_0 and $f_0 + \Delta f$ are neglected and included, respectively (from [13] with permission, ©2011 Cambridge University Press).*

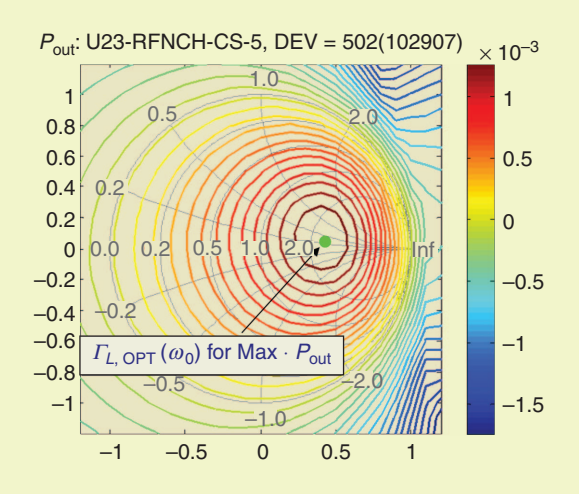

Figure 12. *Constant power contour for a 65 nm metal-oxide semiconductor field-effect transistor (MOSFET). The green dot indicates the point of maximum power (from [13] with permission, ©2011 Cambridge University Press).*

Large-signal measurements can be conducted with the multiple recording scheme with increased time resolution.

by the transistor for a single output power level can map a wide region of the IV characteristics as is demonstrated in Figure 15. Note that the inset figure in Figure 15 shows the loci of the output reflection coefficient during real-time active-load-pull. Using such large-signal measurements, the direct extraction of the nonlinear device model (IV characteristic and device charges) has also been reported [25]–[27]. A similar effect was also reported using multisine excitations [3], [28] and used for the development of behavioral models.

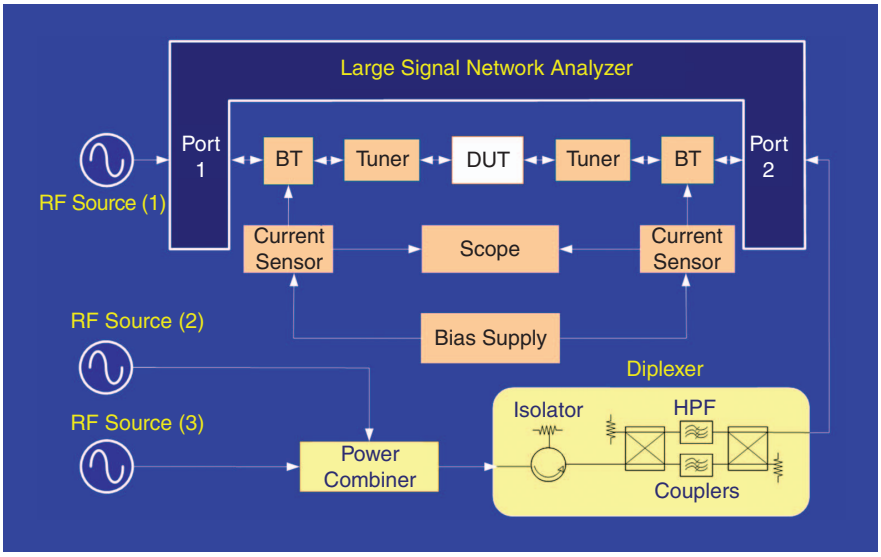

Figure 13. *Test bed used for real-time active-load-pull measurements.*

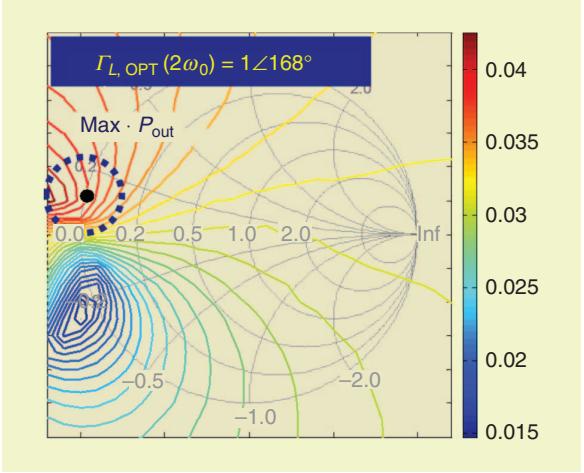

Figure 14. *Real-time active-load-pull at the second harmonic for the optimization of the output power of a negative resistance [24].*

Pulsed-RF Real-Time Active-Load-Pull

As we have seen, the multiple recording technique allows the acquisition of periodic pulsed RF signals with zero desensitization because the pulsed signal is only measured for a short duration when the RF power is applied. Multiple recordings can also be used to acquire signals which are both pulsed and modulated [28]. As a result, ultrafast real-time active load-pull can now also be used to characterize the nonlinear response of transistors driven by pulsed-RF, pulsed-bias signals.

As an example, results of a pulsed-RF, real-time active-load-pull for an on-wafer GaN transistor are shown in Figure 16. Both the output power and input power are swept in the real-time active-load-pull measurement to generate the 1dB gain compression contour and associated P1dB output power shown in Figure 16(a) and (b), respectively. Note that the peak gain at 1dB compression occurs in an unstable region, whereas the peak P1dB output power takes place in a stable region. Note also that for each input power level, 14 different output power levels were measured. The P1dB calculations were then based on 16 different input power levels. Overall, $14 \times 16 = 224$ measurements were performed by the LSNA. For CW load-pull measurements, the acquisition time for each measurement is typically of 10 ms. The limitation for these CW measurements becomes, then, the signal processing done by the computer that is managing the measurements, rather than the sampler-based NVNA measurements themselves. For pulsed-RF measurements, the measurement duration will be longer and depend on the duty cycle. Nevertheless, the resulting pulsed-RF real-time active-load-pull can greatly reduce the measurement time and accelerate the design of pulsed-RF power amplifiers compared to the pulsed-RF active load-pull technique [30].

Conclusion

In this article, we have reviewed various advanced broadband and pulsed measurement techniques which have been developed for sampler-based NVNAs. We have seen that the RF modulation capability of sampler-based NVNAs was not limited by the IF bandwidth of its receiver. Two methods for pulsed-RF, pulsed-bias measurements were also presented. The method based on the concept of multiple recordings enables one to achieve pulsed-RF measurements with 0 dB

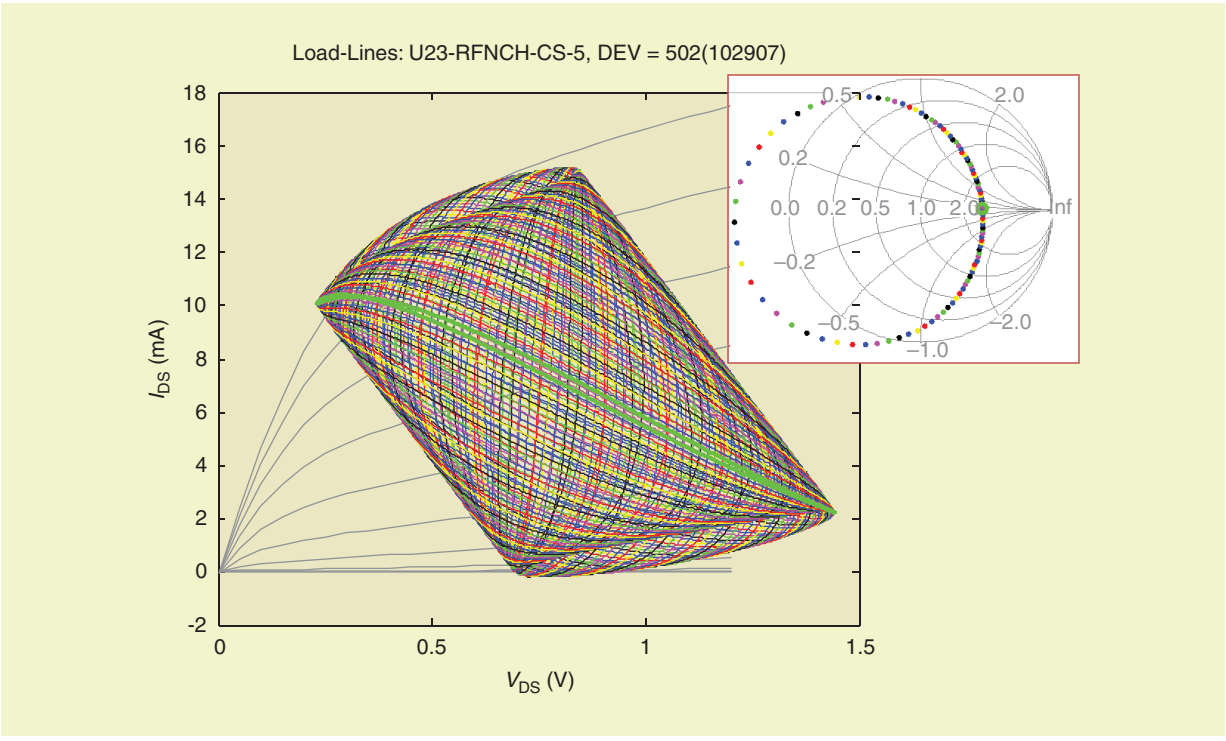

Figure 15. *The load-line experienced by a complementary metal-oxide semiconductor field-effect transistor (CMOSFET) during the 10 ms real-time active-load-pull measurement. The inset indicates the reflection coefficient swept by a single large-signal network analyzer measurement. The green load line corresponds to the impedance termination (green dot on the inset) providing maximum output power in Figure 12.*

desensitization (no dynamic range degradation) even for very low duty cycles. Real-time active load-pull techniques for the rapid design of microwave power amplifiers were also presented. Finally, it was demonstrated that pulsed-RF real-time active-load-pull could also be performed for the rapid design of pulsed-RF PAs or the characterization of transistors with reduced memory effects. These various measurements with sampler-based NVNAs were made possible thanks to the use of advanced ADC triggering techniques.

Due to its inherently wide input bandwidth and its speed of acquisition, the sampler-based NVNA exhibits a smaller dynamic range (typically around 70dB) for CW measurements when compared to high-performance mixer-based NVNAs. Nevertheless, with recently commercialized solutions (VTD, Mesuro), oscilloscope-based and sampler-based NVNAs may offer a lower-cost alternative for large-signal measurements when a dedicated nonlinear test bed is desired.

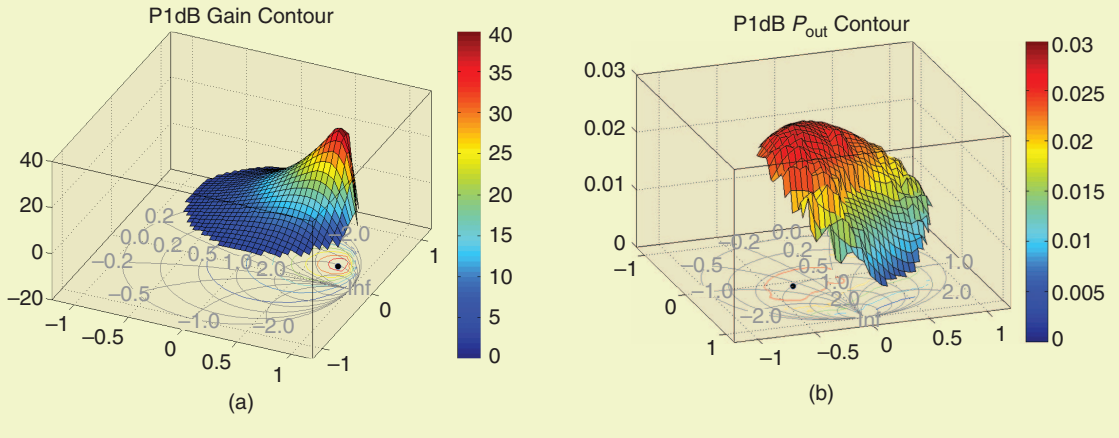

Figure 16. *Contour plots of the P1dB compression gain and P1dB output power obtained from pulsed-RF real-time active load-pull using both input and output power sweeps.*

Acknowledgments

The authors would like to thank the editors Dr. Joe Gering and Dr. Kate Remley for their help with the preparation of this review. Patrick Roblin is also grateful for the inspiration provided along the years by his colleagues at the Automatic RF Techniques Group (ARFTG) including Prof. Dominique Schreurs, Prof. Jean-Pierre Teyssier, Dr. John Wood, Dr. Jan Verspecht, Dr. Kate Remley, Dr. Marc Vanden Bossche, Dr. Dylan Williams, Prof. Johannes Benedikt, Prof. Paul Tasker, Dr. David Root, Prof. Andrea Ferrero, Prof. José Pedro, and their collaborators.

The LSNA research performed at Ohio State University was supported by the National Science Foundation under Grant ECS-0622003. Additional support was provided by the Office of Naval Research under Grant N0014-08-1-0101.

References

[1] J. Verspecht, "Calibration of a measurement system for high frequency nonlinear devices," Doctoral dissertation, Vrije Universiteit Brussel, Elsene, Belgium, Nov. 1995.

[2] J. Verspecht, "Large signal network analysis," *IEEE Microwave Mag.*, vol. 6, pp. 82–92, Dec. 2005.

[3] Y. Ko, P. Roblin, S. Myoung, J. Strahler, F. De Groote, and J. P. Teyssier, "Multi-harmonic broadband measurements using an large signal network analyzer," in *75th ARFTG Conf. Dig.*, Anaheim, CA, June 2010, pp. 1–6.

[4] K. A. Remley, "Multisine excitation for ACPR measurements," in *IEEE MTT-S Int. Microwave, Symp. Dig.*, Philadelphia, PA, June 2003, pp. 2141–2144.

[5] J. Verspecht, "Broadband measurements for wireless telecommunication systems," in *62nd ARFTG Conf. Dig.*, Washington, DC, Dec. 2005. [Online]. Available: http://www.arftg.org/conferences/arftg66/nonlinear_measurements_workshop.pdf

[6] K. A. Remley, D. Schreurs, D. Williams, and J. Wood, "`Extended NVNA bandwidth for long-term memory measurement," in *IEEE MTT-S Int. Microwave, Symp. Dig.*, Fort Worth, TX, June 2004, pp. 1739–1742.

[7] M. E. Yaagoubi, G. Neveux, D. Barataud, T. Reveyrand, J.-M. Nébus, F. Verbeyst, F. Gizard, and J. Puech, "Time-domain calibrated measurements of wideband multisines using a large-signal network analyzer," *IEEE Trans. Microwave Theory Tech.*, vol. 56, no. 5, pp. 1180–1192, May 2008.

[8] F. De Groote, J.-P. Teyssier, T. Gasseling, O. Jardel, and J. Verspecht, "Introduction to measurements for power transistor characterization," *IEEE Microwave Mag.*, vol. 9, no. 3, pp. 70–85, June 2008.

[9] I. Suh, P. Roblin, Y. Ko, C.-K. Yang, A. Malonis, A. Arehart, S. Ringel, C. Poblenz, Y. P. Speck, and U. Mishra, "Additive phase noise measurements of AlGaN/GaN HEMTs using a large signal network analyzer and tunable monochromatic light source," in *74th ARFTG Conf. Dig.*, Boulder, CO, Dec. 2009, pp. 1–5.

[10] A. S. Roy and C. C. Enz, "Analytical modeling of large-signal cyclo-stationary low-frequency noise with arbitrary periodic input," *IEEE Trans. Electron Devices*, vol. 54, no. 9, pp. 2537–2545, Sept. 2007.

[11] S. J. Doo, P. Roblin, S. Lee, D. Chaillot, and M. V. Bossche, "Pulsed-IV pulsed-RF measurements using a large signal network analyzer," in *65th ARFTG Conf. Dig.*, Long Beach, CA, June 2005, pp. 1–7.

[12] S. J. Doo, P. Roblin, V. Balasubramanian, R. Taylor, K. Dandu, J. Strahler, G. H. Jessen, and J.-P. Teyssier, "Pulsed active load–pull measurements for the design of high-efficiency class-B RF power amplifiers with GaN HEMTs," *IEEE Trans. Microwave Theory Tech.*, vol. 57, no. 4, pp. 881–889, 2009.

[13] P. Roblin, *Nonlinear RF Circuits and Nonlinear Vector Network Analyzers*. Cambridge, U.K.: Cambridge Univ. Press, to be published.

[14] P. McGovern, J. Benedikt, P. J. Tasker, J. Powell, K. P. Hilton, J. L. Glasper, R. S. Balmer, T. Martin, and M. J. Uren, "Analysis of DC-RF dispersion in AlGaN/GaN HFET's using pulsed I-V and time-domain waveform measurements," in *IEEE MTT-S Int. Microwave, Symp. Dig.*, Long Beach, CA, June 2005, pp. 1–4.

[15] S. J. Doo, P. Roblin, G. H. Jessen, R. C. Fitch, J. K. Gillespie, N. A. Moser, A. Crespo, G. Simpson, and J. King, "Effective suppression of IV knee walk-out in AlGaN/GaN HEMTs for pulsed-IV pulsed-RF with a large signal network analyzer," *IEEE Microwave Wireless Comp. Lett.*, vol. 16, no. 12, pp. 681–683, Dec. 2006.

[16] J. P. Teyssier, C. Charbonniaud, D. Barataud, M. Nébus, and R. Quéré, "Large-signal time-domain characterization of microwave transistors under RF pulsed conditions," in *60th ARFTG Nonlinear Measurements Workshop*, Washington, DC, Dec. 2002. [Online]. Available: http://www.arftg.org/conferences/arftg60/nonlinear_measurements_workshop.pdf

[17] F. De Groote, O. Jardel, T. Reveyrand, J.-P. Teyssier, and R. Quéré, "Very small duty cycles for pulsed time domain transistor characterization," in *Proc. 37th EuMC*, vol. 4, June 2008, pp. 112–117.

[18] J. Faraj, F. De Groote, J.-P. Teyssier, J. Verspecht, R. Quéré, and R. Aubry, "Pulse profiling for AlGaN/GaN HEMTs large signal characterizations," in *Proc. 38th EuMC*, Amsterdam, The Netherlands, Oct. 2008, pp. 757–760.

[19] C. K. Yang, P. Roblin, F. D. Groote, J. P. Teyssier, S. Ringel, C. Poblenz, Y. Pei, J. Speck, and U. Mishra, "Pulsed-IV pulsed-RF cold-FET parasitic extraction of biased AlGaN/GaN HEMTs using large signal network analyzer," *IEEE Trans. Microwave Theory Tech.*, vol. 58, no. 5-I, pp. 1077–1088, 2010.

[20] F. Verbeyst and M. Vanden Bossche, "Real-time and optimal PA characterization speeds up PA design," in *Proc. 34th EuMC*, Amsterdam, The Netherlands, Oct. 2004, pp. 431–434.

[21] S. C. Cripps, *RF Power Amplifiers for Wireless Communications*, 2nd ed. Norwood, MA: Artech House, 2006.

[22] X. Cui, S. J. Doo, P. Roblin, G. H. Jessen, R. G. Rojas, and J. Strahler, "Real-time active load-pull of the 2nd and 3rd harmonics for interactive design of non-linear power amplifiers," in *68th ARFTG Conf. Dig.*, Boulder, CO, Nov. 2006, pp. 1–8.

[23] X. Cui, S. J. Doo, P. Roblin, J. Strahler, and R. G. Rojas-Teran, "High efficiency RF power amplifier designed with harmonic real-time active load-pull," *IEEE Microwave Wireless Comp. Lett.*, vol. 18, no. 4, pp. 266–268, Apr. 2008.

[24] I. Suh, S. J. Doo, P. Roblin, X. Cui, Y. G. Kim, J. Strahler, M. V. Bossche, R. Rojas, and H. D. Park, "Negative input resistance and real-time active load-pull measurements of a 2.5 GHz oscillator using an LSNA," in *69th ARFTG Conf. Dig.*, Honolulu, HI, June 2007.

[25] M. C. Curra-Francos, P. J. Tasker, M. Fernandez-Barciela, Y. Campos-Roca, and E. Sanchez, "Direct extraction of nonlinear FET Q-V functions from time domain large signal measurements," *IEEE Microwave Guided Wave Lett.*, vol. 10, no. 12, pp. 531–533, Dec. 2000.

[26] D. Schreurs, J. Verspecht, S. Vandenberghe, and E. Vandamme, "Straightforward and accurate nonlinear device model parameter-estimation method based on vectorial large signal measurements," *IEEE Trans. Microwave Theory Tech.*, vol. 50, no. 10, pp. 2315–2319, Oct. 2002.

[27] D. Schreurs and K. A. Remley, "Use of multisine signals for efficient behavioral modeling of RF circuits with short-memory effects," in *61st ARFTG Conf. Dig.*, June 2003, pp. 65–72.

[28] Y. Ko, P. Roblin, "Broadband multsine NVNA measurements for identification of memory effects," Workshop on Nonlinear measurements to investigate memory effects of RF transistors and active devices, at ARFTG 76th Symposium, Clearwater Beach, Florida, Dec. 2010. [Online] Available: http://www.arftg.org/conferences/arftg76/WS_F2010_NL_MEMORY_Brochure.pdf

[29] F. De Groote, P. Roblin, J. P. Teyssier, C. Yang, S. Doo, and M. Vanden Bossche, "Pulsed multi-tone measurements for time domain load pull characterizations of power transistors," in *73th ARFTG Conf. Dig.*, Boston, MA, May 2009.

[30] S. J. Doo, P. Roblin, V. Balasubramanian, R. Taylor, K. Dandu, J. Strahler, G. H. Jessen, and J.-P. Teyssier, "Pulsed-IV pulsed-RF active load-pull measurements for the design of high-efficiency class-B RF Power amplifiers with GaN HEMTs," *IEEE Trans. Microwave Theory Tech.*, vol. 57, no. 4, pp. 881–889, Apr. 2009.